Forschung im Ingenieurwesen
https://doi.org/10.1007/s10010-023-00695-2

ORIGINALARBEITEN/ORIGINALS

Gear skiving with minimum twist errors

Modeling and optimization of flank twist in gear skiving

Andreas Hilligardt[1] · **Volker Schulze**[1]

Received: 31 March 2023 / Accepted: 7 July 2023
© The Author(s) 2023

Abstract
Over the last 15 years, gear skiving has established itself as a highly productive gear cutting process for the production of internal gears and gears with near interference contours. As with all processes with crossed axes, gear skiving generally results in a pronounced natural twist when gears with lead crowning or other flank modifications are produced. In practical applications, the unintended profile angle changes over the tooth width resulting from the twist leading to unwanted contact patterns and unfavorable NVH behavior. In this work, a contact line-based method for tool profile calculation for gear skiving is developed based on conical-screw gear theory. The relationship between contact line and natural twist errors is worked out. The process and tool design strategies for minimizing the twist are elaborated and finally, an adaptive process kinematics for low-twist error gear skiving is presented.

Verschränkungsarmes Wälzschälen

Modellierung und Optimierung der Verschränkung beim Wälzschälen

Zusammenfassung
In den letzten 15 Jahren hat sich das Wälzschälen von Zahnrädern als hochproduktives Verzahnverfahren für die Herstellung von Innenverzahnungen und Zahnrädern mit nahliegender Störkontur etabliert. Wie bei allen Verfahren mit gekreuzten Achsen kommt es beim Wälzschälen in der Regel zu einer ausgeprägten natürlichen Verschränkung, wenn Zahnräder mit Flankenmodifikationen hergestellt werden. In der Praxis führen die aus der Verschränkung resultierenden ungewollten Profilwinkeländerungen über die Zahnbreite zu unerwünschten Tragbildern und ungünstigem NVH-Verhalten. In dieser Arbeit wird auf Basis des Konus-Schraubradgetriebes eine berührlinienbasierte Methode zur Werkzeugkonturberechnung für das Wälzschälen erarbeitet. Der Zusammenhang zwischen Berührlinie und natürlicher Verschränkung wird aufgearbeitet. Es werden Prozess- und Werkzeugauslegungsstrategie zur Minimierung der Verschränkung abgeleitet und abschließend eine adaptive Prozesskinematik für das verschränkungsarme zweiflankige Wälzschälen mit geeigneten Werkzeugen präsentiert.

1 Introduction

Global energy and climate targets and the shortage of raw materials require advances in energy efficiency and material utilization. At the same time, the limited space available for mobile applications places the focus of development on increasingly compact drive units with the highest power density. Due to high power density and good efficiencies at high transmission ratios, planetary gearboxes are increasingly used in drive units [1]. While internal gears of a DIN Q10 quality are still sufficient for combustion engine-driven transmission solutions, internal gears of DIN Q6 qualities are required for electrical powertrains [2]. Through continuous further development, gear skiving can now produce internal gearing of such quality in finishing. Gear skiving is characterized by high productivity and flexibility in

✉ Andreas Hilligardt
andreas.hilligardt@kit.edu

Volker Schulze
volker.schulze@kit.edu

[1] wbk Institute of Production Science, Karlsruhe Institute of Technology, Kaiserstr. 12, 76131 Karlsruhe, Germany

Published online: 26 July 2023

the production of internal gears. For example, main times of only 10 s can be achieved for the hard-fine machining of automotive internal gears by hard skiving [3]. To improve the contact pattern and the noise behavior, gears are usually designed with lead modifications [4]. During the manufacturing of these modifications, most processes and strategies result in twist-like deviations between flank nominal and actual geometry [5], which reduce Load capacity and NVH behavior. For generating grinding, profile grinding, gear hobbing, shaving, and honing, methods of process control or tool geometry adjustment have been successfully developed to minimize twist errors of external gears. To improve the performance and noise characteristics of upcoming planetary gear generations, lead-modified internal gears offer high potential, but require a suitable manufacturing process. Due to its flexibility and highest productivity, gear skiving would be an economically ideal solution for the production of such internal gears. But the manufacturing of lead crowning, the formation of twist errors, and solutions to minimize them have not yet been sufficiently studied for gear skiving.

2 State of the art

Twist errors occur in a variety of gear manufacturing processes during the manufacturing of lead modifications. The deviations between nominal and actual geometry, also known as bias errors, present themselves as an uneven profile and flank geometry across the width of the manufactured gear [5], see Fig. 1. This leads to a profile angle deviation $f_{H\alpha}$ across the tooth width. The phenomenon occurs particularly with the execution of flank modifications [5]. This is due to the fact that in most gear manufacturing processes for helical gears, the line of contact between the workpiece and the tool runs not exclusively through the workpiece transverse section. This is the case, for example, with generating grinding [6] and gear hobbing [7]. Due to the contact line running obliquely across the flank, the tooth tip and root of the workpiece are produced by different relative tool height positions according to the tool axial feed [6]. Therefore, if the flank modification is produced by changing the center distance across the width of the workpiece, different center distances are present at the time of workpiece tooth tip and tooth root production, resulting in twist errors, see Fig. 1. The desired flank topology is achieved only on one flank line. Twist errors increase in generating grinding with rising flank modification and workpiece helix angle [6]. The exact quantification of twist errors is usually done by numerically based geometric simulations [8]. To minimize twist errors, the pitch and the pressure angle of the tool are specifically changed over the tool width during diagonal gear hobbing or generating grinding with continuous shifting in tool width over the workpiece width [6]. The combination of tool profile modification and process control creates a twist that counteracts the natural twist error. This technology also enables the targeted imprinting of a twist on the workpiece. In addition to the dressing or external production of the correspondingly variable tool profiles, precise synchronization and control of the NC axes are required for this technology. In the last 15 years, low-twist generating grinding has been widely used.

The general gear skiving process is a cross-axis process with a geometrically defined cutting edge, in which the tool can be positioned off-center to create an effective clearance angle. In this context, gear skiving is also characterized by a contact line that runs obliquely over the workpiece flank, which, in contrast to generating grinding, also applies in particular to workpieces with straight teeth. A contact line-based tool profile calculation for gear skiving was developed in [11]. Up to now, only the consid-

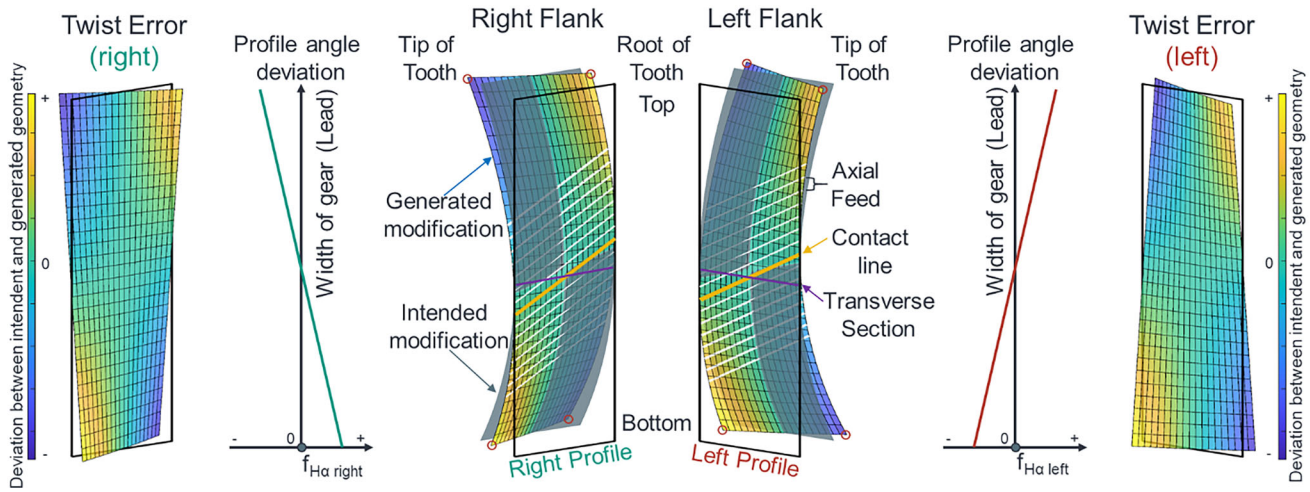

Fig. 1 Flank twist in a tooth space manufactured with a lead crowning

eration of constructive tool angles is missing. Furthermore, gear skiving is characterized by the possibility of workpiece profile adaptations by a targeted change in the kinematics [16]. Simulative approaches have become established for the calculation of these relationships and the complex cutting conditions of gear skiving. OpenSkiving represents an Open-Source-Software for kinematics, tool profile, topography and cutting condition calculation [14].

3 Kinematics of gear skiving

The basic kinematics of gear skiving can be calculated based on a profile-shifted conical helical gear pairing. This has already been discussed in [9] and will be summarized in the following due to its importance for this work. The basic assumption of this approach is the mathematical consideration of the tool as a conical gear, while it is cylindrically realized, see Fig. 2a. In the special case of centered gear skiving, the tool is mathematically considered as a heli-

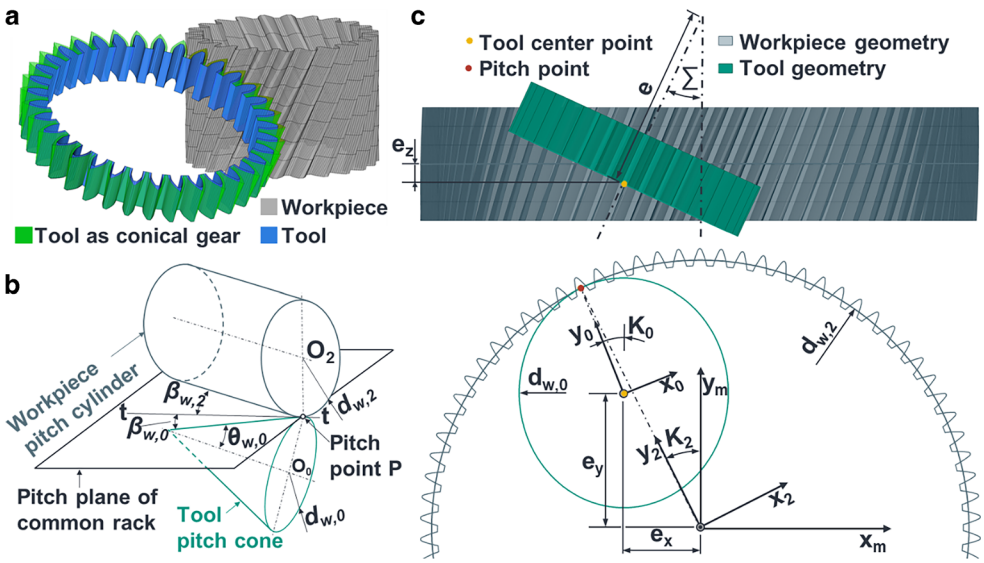

Fig. 2 (**a**) Mathematical and real tool designs for gear skiving. (**b**) Working pitch geometries of the generating gear. (**c**) Process kinematics of internal gear skiving

Table 1 Input and output parameters of the kinematics calculation

Input		Output	
Workpiece normal pressure angle	α_n	Working transverse pressure angles	$\alpha_{wt,0(2)}$
Workpiece normal module	m_n	Working pitch circles	$d_{w,0(2)}$
Workpiece generating addendum modification coefficient	$x_{E,2}$	Working helix angles	$\beta_{w,0(2)}$
Tool addendum modification coefficient	x_0	Working cone angle (Effective tip relief angle)	θ_w (α_{ea})
Tool/Workpiece number of teeth	$z_{0(2)}$	Effective cross-axis angle	$\sum_e$
Tool/Workpiece helix angle	$\beta_{0(2)}$	Machine cross-axis angle	$\sum$
Tool cone angle	θ_0	Tool center point position	$e_{x\,(y)\,(z)}$

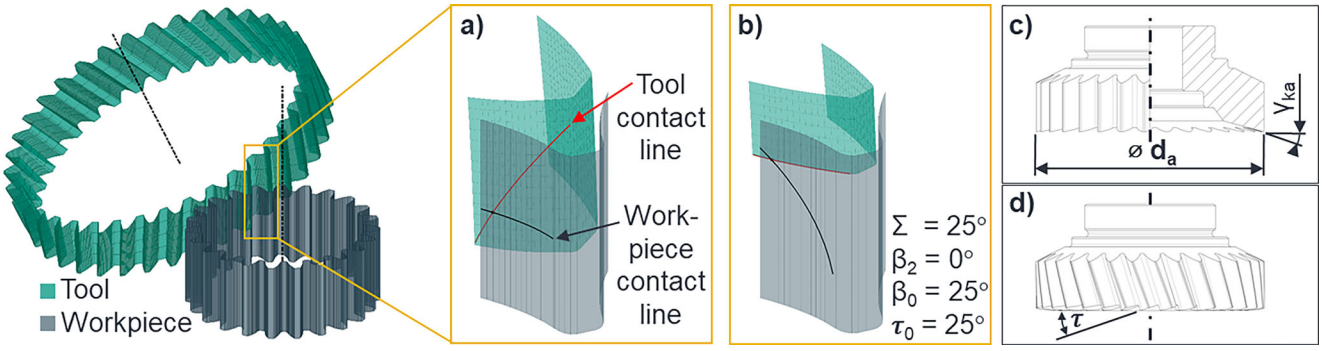

Fig. 3 Contact line in *a)* conical gear drive and *b)* gear skiving [9], and *c)* constructive tip rake angle as well as *d)* stair angle on a skiving tool

cal gear and is realized as upward tapered gear, to achieve a clearance angle.

This approach allows the process kinematics to be calculated directly for a given workpiece and a skiving tool predefined by its gear parameters, see Table 1. The calculation is based on the condition of backlash-free tooth engagement in the working pitch plane. With an identical normal module m_n and normal pressure angle α_n of tool and workpiece, the transverse pressure angle $\alpha_{tR(L),0}$ of the right and left tool flanks can be evaluated according to Eq. 1 with the sign term of the number of workpiece teeth $z_2/|z_2|$ for internal toothed workpieces, the working normal pressure angle α_{wn} of the common working rack, the tool working helix angle $\beta_{w,0}$, and the working cone angle $\theta_{w,0}$. For the working transverse pressure angle $\alpha_{wt,2}$ of the helical workpiece, the expression simplifies.

$$\begin{aligned}\tan\left(\alpha_{wtR(L),0}\right) = &\frac{\tan\left(\alpha_{wn}\right)}{\cos\left(\beta_{w,0}\right)} \cdot \cos\left(\theta_{w,0}\right) \\ &\mp \frac{z_2}{|z_2|}\tan\left(\beta_{w,0}\right) \cdot \sin\left(\theta_{w,0}\right)\end{aligned} \tag{1}$$

$$\tan\left(\alpha_{wt,2}\right) = \tan\left(\alpha_{wn}\right) / \cos\left(\beta_{w,2}\right) \tag{2}$$

The ratio of pitch circle and working pitch circle can be expressed by the transverse factor of pressure angles $\xi_{t,0(2)}$. For the workpiece, this factor also gives the working workpiece helix angle $\beta_{w,2}$ through the definition of the base helix angle. Furthermore, the ratio of the pitch circles $d_{0(2)}$ and the working pitch circles $d_{w,0(2)}$ can be expressed through $\xi_{t,0(2)}$.

$$\begin{aligned}\xi_{t,0} &= \cos\left(\alpha_{wtL,0}\right) / \cos\left(\alpha_{tL,0}\right) \\ &= \cos\left(\alpha_{wtR,0}\right) / \cos\left(\alpha_{tR,0}\right)\end{aligned} \tag{3}$$

$$\xi_{t,2} = \cos\left(\alpha_{wt,2}\right) / \cos\left(\alpha_{t,2}\right) = \tan\left(\beta_2\right) / \tan\left(\beta_{w,2}\right) \tag{4}$$

$$d_{w,0(2)} = d_{0(2)}/\xi_{t,0(2)} = \left(z_{0(2)} m_n\right) / \left[\xi_{t,0(2)} \cos\left(\beta_{0(2)}\right)\right] \tag{5}$$

The condition of a backlash-free tooth meshing between workpiece and tool can be expressed for gear skiving with the involute function inv, tool teeth z_0, workpiece teeth z_2, the workpiece generation profile shift factor $x_{E,2}$, and the profile shift of the tool x_0.

$$\begin{aligned}&\frac{z_0}{2}\left[\text{inv}\left(\alpha_{wtL,0}\right) + \text{inv}\left(\alpha_{wtR,0}\right) - \text{inv}\left(\alpha_{tL,0}\right)\right. \\ &\left.-\text{inv}\left(\alpha_{tR,0}\right)\right] + z_2\left[\text{inv}\left(\alpha_{wt,2}\right) - \text{inv}\left(\alpha_{t,2}\right)\right] \\ &= 2 \cdot \tan\left(\alpha_n\right)\left[x_0 \cos\left(\theta_0\right) + x_{E,2}\right]\end{aligned} \tag{6}$$

By the coupled solving of Eqs. 1–6, the working variables can be evaluated. From this, the installation sizes of the tool can be derived for the kinematics definition of gear skiving process. The installation sizes are shown in Fig. 2c. The working cone angle corresponds to the theoretical effective tip relief angle α_{ea}, so from its definition [10], the tool position angle K_0 can be derived. The effective cross-axis angle $\sum_e$ results from the sum of the working helix angles of workpiece $\beta_{w,2}$ and tool $\beta_{w,0}$. Through the combination of effective cross-axis angle and working cone angle, the absolute machine cross-axis angle $\sum$ arises.

$$\tan\left(\theta_{w,0}\right) = \frac{2 \cdot \sin\left(\theta_0\right)\tan\left(\alpha_n\right)}{\xi_{t,0}\cos\left(\beta_0\right)\left[\tan\left(\alpha_{wtL,0}\right) + \tan\left(\alpha_{wtR,0}\right)\right]} \tag{7}$$

$$\tan\left(\theta_{w,0}\right) = \tan\left(\alpha_{ea}\right) = \frac{z_2}{|z_2|}\tan\left(-\Sigma\right) \cdot \sin\left(K_0\right) \tag{8}$$

$$\Sigma_e = -\left(\beta_{w,0} + \beta_{w,2}\right) \tag{9}$$

$$\Sigma = \frac{\Sigma_e}{|\Sigma_e|}\arccos\left[\cos\left(\theta_{w,0}\right) \cdot \cos\left(\Sigma_e\right)\right] \tag{10}$$

The tool center point position $e_{x\,(y)\,(z)}$ results from the further analysis of workpiece working pitch cylinder and

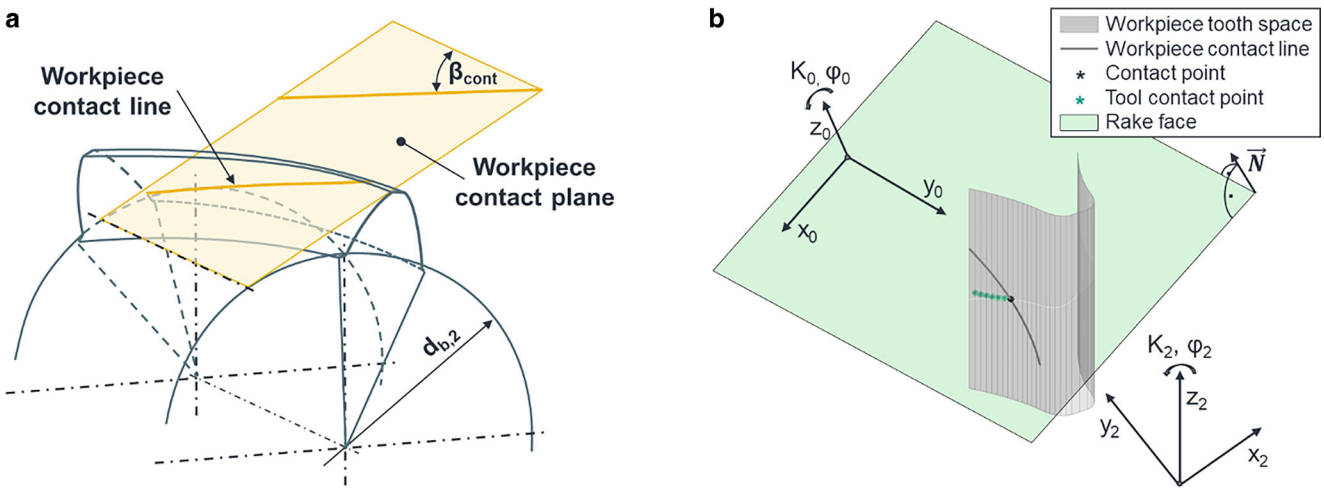

Fig. 4 (**a**) Contact line of a helical workpiece in analogy to [12]. (**b**) Contact in rake face

the tool's working pitch cone position related to the pitch plane of the common rack, see Fig. 2b.

$$e_x = \frac{z_2}{|z_2|}\sin(\Sigma)\left[\frac{d_{w,2} + \frac{z_2}{|z_2|}d_{w,0}\cos(\theta_{w,0})}{2\cdot\sin(\theta_{w,0})} - \frac{e_y\tan(\Sigma_e)}{\tan(\Sigma)\sin(\theta_{w,0})}\right] \tag{11}$$

$$e_y = \frac{\Sigma_e}{|\Sigma_e|}\frac{\sin(\Sigma_e)}{2\cdot\sin(\Sigma)}\left[\frac{z_2}{|z_2|}d_{w,0} + d_{w,2}\cdot\cos(\theta_{w,0})\right] \tag{12}$$

$$e_z = \frac{z_2}{|z_2|}\cdot\sin(\Sigma)\cdot\sin(K_0)\cdot\frac{d_{w,0}}{2} \tag{13}$$

4 Tool profile and contact line

The point contact between two gears in a conical helical gear pairing generally runs along an oblique contact line across the flanks, see Fig. 3 a). This contact situation is not permissible for machining with a geometrically defined cutting edge. Here, all contact points must lie in the rake face. For gear skiving, this means that all tools for which the helix and/or cone angle is not zero and the actual contact line would therefore not lie in the rake face require a specific profile modification to shift the contact line into the rake face, see Fig. 3 b). Since the kinematic calculation using the conical helical gear pairing is based on the condition of backlash-free tooth meshing on the working pitch circles, it follows that the tooth thickness on the working pitch circle is exact and the line of meshing passes through this point. The further contour of the tool profile can be determined by solving the three-dimensional basic requirement of a gear tooth system [11]. Alternatively, only one further point of the tool profile can be calculated and from this, a profile crowning around the working pitch circle of the tool profile can be derived concerning the ideal involute of the conical gear [9]. This method is initially limited to tools without constructive tip rake angle γ_{ka} and without stair angle τ.

A generalized method for tool profile calculation can be derived from the workpiece contact line. If the course of the contact line along the workpiece is known, the workpiece contact points can be transferred to the tool coordinate system, considering the process kinematics. The inclination of the contact line on the workpiece flank can be described

Table 2 Workpiece, tool, and process data of example 1

Workpiece data					
Number of teeth	z_2	–103	Normal pressure angle	α_n	17.5°
Helix angle	β_2	20.8°	Normal module	m_n	1.16 mm
Tip diameter	d_{a2}	128.1 mm	Generating addendum modification coefficient	x_E	–1.73
Root diameter	d_{f2}	134.5 mm	Tooth width	b_2	25 mm
Root form d	d_{Ff2}	134.1 mm	Tip form diameter	d_{Fa2}	128.54 mm
Tool and process data					
Number of teeth	z_0	63	Constructive tip clearance angle	α_{ka}	0°
Helix angle	β_0	11.6°	Constructive tip rake angle	γ_{ka}	–15°
Working pitch d	d_{w0}	76.63 mm	Stair angle	τ	11.6°
Cone angle	θ_0	10°	Cross-axis angle	Σ	–12.5°

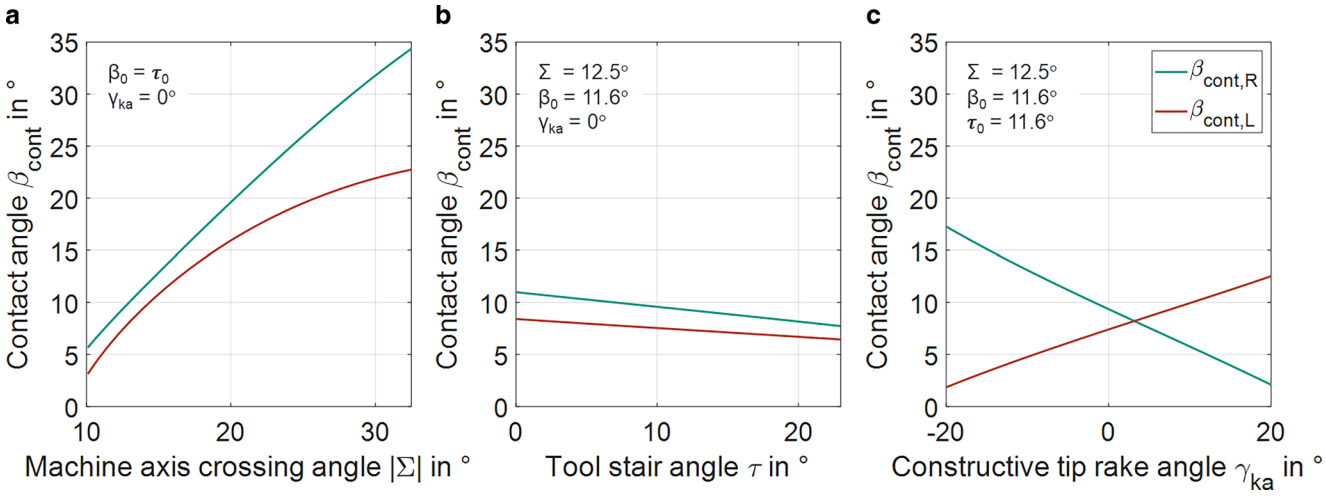

Fig. 5 Analysis of the contact angle via (**a**) cross-axis angle, (**b**) stair angle, and (**c**) constructive tip rake angle

by its helix angle on the workpiece base cylinder β_{cont}, see Fig. 4a. For any point on the involute of the workpiece with the face coordinates x and y, the axial position z is thus obtained based on the engagement distance. For gear skiving, a distinction between left and right flanks is necessary here, since the contact angles are generally not identical. If the skiving tool is designed with a stair angle, the axial position in the working pitch circle is shifted by an axial offset z_{cont}. For helical geared workpieces, the rotation of the transverse section coordinates along the helix with the axial position must be considered.

$$z = \frac{\sqrt{2\sqrt{x^2+y^2}-d_{b,2}^2}-\sqrt{d_{w,2}^2-d_{b,2}^2}}{2\cdot\cos\left(\beta_{b,2}\right)} \cdot \sin\left(\beta_{\mathrm{cont},L(R)}\right) + z_{\mathrm{cont},L(R)} \tag{14}$$

By solving the three-dimensional gearing law at two workpiece flank points, the contact angle β_{cont} and axial offset z_{cont} can be calculated for each flank. With this information, no further computationally intensive point-by-point solution of the gearing law is necessary. The workpiece involute points along the contact line need only be transferred to the tool coordinate system. From the normal form of the rake face it can be deduced that the contact points lie within the rake face if the scalar product of the difference between the involute point and the rake face support point on the working pitch cycle as well as the rake face normal $\vec{N}$ is equal to zero in the meshing position.

$$\left(\begin{pmatrix} x_{\varphi 2} \\ y_{\varphi 2} \\ z_{\varphi 2} \end{pmatrix} - \begin{pmatrix} \sin(\sum) \\ 0 \\ \cos(\sum) \end{pmatrix} \frac{d_{w,0}\tan(\gamma_{ka})}{2}\right) \cdot \overrightarrow{N_{\varphi 0}} = 0 \tag{15}$$

With the resulting workpiece and tool meshing angles φ_2 and φ_0 the workpiece profile can be mapped in to the tool coordinate system, as indicated in Fig. 4b.

5 Contact angle dependence of natural twist errors

As shown in Fig. 1, a contact line inclined over the workpiece flank when producing a lead modification by exclusively adapting the center distance or, in the case of single-flank machining, by exclusively adapting the coupling angle between the workpiece and the tool, inevitably results in twist errors. This is because the path control can only be adjusted to the lead line on one diameter. Due to the inclined contact line, the other diameters are machined in a correspondingly offset manner, resulting in twist errors.

With the engagement distance between the tip and root-forming circle of the workpiece d_{Fa} and d_{Ff}, the maximum profile angle error $\Delta f_{H\alpha}$ at the tooth edges for a symmetric square lead crowning c_β over the gear width b can be determined as a function of the contact angle β_{cont}.

$$|\Delta f_{H\alpha}| = \left|\frac{\sqrt{d_{\mathrm{Fa},2}^2-d_{b,2}^2}-\sqrt{d_{\mathrm{Ff},2}^2-d_{b,2}^2}}{2\cdot\cos\left(\beta_{b,2}\right)}\right| \cdot \sin\left(\beta_{cont,L(R)}\right)\cdot\frac{4c_\beta}{b} \tag{16}$$

6 Case study on the main influencing variables of the contact angle in gear skiving

For the example internal gearing and example gear skiving process summarized in Table 2, the influence of the kinematics design and the constructive tool sizes on the angle β_{cont} of inclination of the contact line on the workpiece flank was investigated. First, the influence of the cross-axis angle was investigated by varying the tool helix angle while keeping the tool profile shift constant, see Fig. 5a. As it is generally the case in industrial practice, the stair angle was selected to be the same as the helix angle. Due to the tool cone angle and the resulting off-center process, asymmetric contact angles occur on the left and right workpiece flanks. As the cross-axis angle decreases, the contact angles drop significantly. In the next step, the influence of the stair angle was detached at a constant cross-axis angle and constructive tip rake angle, see Fig. 5b. Only a low sensitivity of the contact angles to the tool stair angles is shown. Finally, the influence of the constructive tip rake angle was investigated. This has a considerable influence on the inclination of the contact line. While the contact angle on the left flank increases with increasing constructive tip rake angle, that of the right flank decreases. here is thus an opposite influence, see Fig. 5c.

7 Tool design for twist error minimization

As can be seen from Eq. 16, the twist error correlates directly with the contact angle. To minimize the twist error with classical process control, the contact angle must be minimized. As can be seen from Fig. 5, this can be achieved primarily by reducing the cross-axis angle. The constructive tip rake angle results in an opposite change of the contact angle on the left and right flank. Thus, the constructive tip rake angle can minimize the contact angle only on one preferred flank. The effect of the stair angle is small. This is

therefore primarily used for symmetrical adjustment of the cutting conditions and in particular the effective rake angle.

Reducing the cross-axis angle is initially the most effective method. However, for gear skiving with tooth root machining, gear skiving with small cross-axis angles leads to significantly lower effective rake angles in the tool tip area due to the significantly more curved tool trajectories, and this results in increased tool wear [13]. Reducing the cross-axis angle in this case, therefore, has a negative effect on the process economic efficiency. In the flank area, the effect of the reduction of the cross-axis angle is less pronounced, so processes with a cross-axis angle of up to 10° are often still feasible for pure flank machining in a finishing or hard finishing operation. The lower axial feeds required for smaller cross-axis angles for the maximum chip thickness and feed marks to keep within the limits are compensated here by the higher rotational speeds to achieve the identical cutting speed and reduced in- and outrun required. Hence, these processes can also compete with finishing and hard finishing processes with higher cross-axis angles in terms of process times. With smaller cross-axis angles, the cutting lengths are significantly reduced, so that the chip shapes differ.

Many modern gears have helix angles between 10 and 25°. In this case, tools without helix and stair angles can be manufactured for gear skiving, resulting in cross-axis angles of identical order of magnitude. This range is very favorable for soft machining and these tools are noticeably cost-effective in manufacturing and reconditioning. For these applications, a reduction of the cross-axis angle is related to a tool helix angle and thus an increase in the complexity of the tool. If the twist errors only need to be low at one flank or only one flank needs a lead crowning, a constructive rake angle in the form of a cost-effective executable taper surface grinding can be used to minimize the contact angle and thus the twist errors on this flank. In the case of single-flank machining, the corresponding other flank can also be machined with deviating or without crowning.

8 Practical validation of tool design using a reference example

To validate the relationships introduced above, the process from Table 2 was realized. The tool was designed with a tip rake angle of –15°. This results in a contact angle of 4.2° on the left flank and 17.15° on the right flank. The process was deliberately carried out with a negative design rake angle. The minimum effective rake angles on the flanks were determined with the open-source gear skiving simulation software OpenSkiving [14]. The minimum rake angles of –23° are still in a range that can be machined [15].

The tool was manufactured as a single-tooth tool, so there is no influence of roundness and pitch errors of the tool to the finished part quality. Finishing was performed on a Pittler PV315 with an axial feed of 0.126 mm per workpiece revolution under compressed air cooling.

The tooth flanks were manufactured with a symmetrical target lead crowning of 33 µm over the gear width of 25 mm. Here, a conventional change of the center distance over the manufactured gear width was used. The pre-machined thin-walled ring gears were clamped in a six-jaw oblique bolt chuck, see Fig. 7b. Measurements of the manufactured gears were performed on a Zeiss Prismo coordinate measuring machine. The evaluation was performed in the 80% range of the tooth width between the tip and root form circles on 14 flank lines.

The unfiltered measured deviations of the manufactured tooth flanks are shown in Fig. 6. The unequal contact angles and the resulting different twist errors are visible. The real contact angles can be calculated using the z-offset along

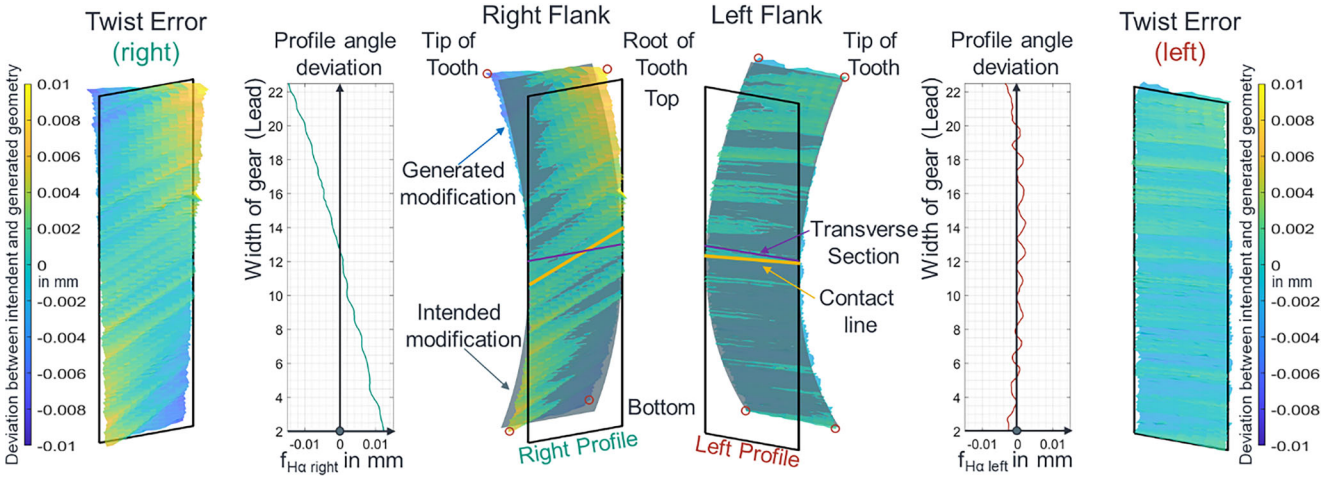

Fig. 6 Experimental twist analysis for the process from Table 2 with a lead crowning of 33 µm

a feed mark and solving Eq. 14 in reverse. This is 4.5° on the left flank and 17.5° on the right flank and thus in good agreement with the design values of 4.2° and 17.15°.

The profile angle errors on the left flank vary between –3 and 2 µm. These variations are primarily due to feed marks and real chip formation. As expected, due to the low left contact angle, no twist can be identified and the target crowning is achieved.

On the right flank, the maximum twist induced profile angle error calculated according to Eq. 16 is 10 µm. The real measured values show twist-related profile angle deviations between –14 and 12 µm, which is in good agreement considering feed marks, tracking errors of machine control and the process-related operational displacements of tool and workpiece.

9 Adaptive process kinematics for twist error minimization

The previously shown reduction of the twist errors through the reduction of the cross-axis angle or the targeted adaptation of the constructive tip rake angle often leads to more complex tools or can minimize the twist errors only on one flank. At the same time, gear skiving offers a high degree of flexibility. Profile angle erros can be compensated by specific adjustment of the off-center, the cross-axis angle and the center distance with suitable tool design, see Fig. 7c. Based on this process freedom, adaptive process kinematics via the tooth width is to be derived in the following for gear skiving to minimize twist errors. A suitable tool design excludes, for example, central tools without constructive rake angle or stair angle, since these tools can only change the profile angle deviation for ring gears into the negative.

For two-flank machining, the kinematics of gear skiving must be corrected so that the profile angle errors on both flanks are corrected simultaneously. The kinematic adaptation can be described by the change of effective tip clearance angle and the effective cross-axis angle.

The variation of the profile angle due to kinematic adaptation can be quantified with known tool profile by the profiling cuts method as it is implemented for gear skiving in the Open-Source-Software OpenSkiving [14]. For the calculation of a targeted process adaptation to correct profile angle deviations, the software contains non-linear parameter optimization based on the least square error of the given and calculated profile angle deviation.

In context of this work, the software was extended by geometric simulation of the entire tooth flank machining for the determination of twist errors. For this purpose, cutting position scar is calculated for each axial feed. The kinematic parameters are adjusted according to the process guidance. The MATLAB®-function "Boundary" is then used to calculate the envelope of all cutting positions and extract the manufactured tooth flanks. By considering the tool tooth entry sequence and tool pitch and runout errors, this method can be used to investigate not only feed marks but also the influence of tool errors on the manufactured flank topography. In particular, this method also allows the calculation of the natural twist errors that occur during gear skiving with conventional adaption of the center distance over the workpiece width to produce lead crowning. From this, the twist-induced profile angle deviations and the necessary kinematic adaption required for correction can be derived over the workpiece width.

The kinematic adaption calculated in this way to compensate the twist-induced profile angle errors can be approximated with high degree of accuracy by a 4th-order approach function for the change of effective tip clearance angle $\Delta\alpha_{ea}$ and the effective cross-axis angle $\Delta\sum_e$.

$$\Delta\alpha_{ea}(b) = a_1 b^4 + a_2 b^3 + a_3 b^2 + a_4 b + a_5 \tag{17}$$

$$\Delta\Sigma_e(b) = s_1 b^4 + s_2 b^3 + s_3 b^2 + s_4 b + s_5 \tag{18}$$

This kinematic adaption results in a process in which the tool center point in all three translational axes, as well as the machine cross-axis angle and the coupling angle of the position control between tool and workpiece are changed over the workpiece width. At the same time, the profile angle deviations resulting from the natural twist are compensated and workpieces with minimized twist errors are manufactured. When designing the kinematic adaptation,

Fig. 7 (**a**) Process setup. (**b**) Six-bolt-chuck. (**c**) Degrees of freedom in gear skiving

Table 3 Tool and process data of example 2

Tool and process data					
Number of teeth	z_0	73	Constructive tip clearance angle	α_{ka}	0°
Helix angle	β_0	0°	Constructive tip rake angle	γ_{ka}	0°
Working pitch d	d_{w0}	86.76 mm	Stair angle	τ	0°
Cone angle	θ_0	10°	Cross-axis angle	Σ	–22.79°

it is important to ensure that the cutting conditions, like local clearance angles, are acceptable. Furthermore, meshing interference, i.e. an impermissible collision between the workpiece flank and the tool clearance face, can occur at the tool exit. This must also be checked before practical implementation, see [10].

10 Practical validation of the adaptive process kinematics

For the previously introduced workpiece, Table 3 shows a process layout with a tool without helix, stair, constructive rake angles and 73 tool teeth. The contact angles are 18.4° on the left flank and 23.22° on the right flank. For the two-flank skiving of a symmetric lead crowning of 18 µm via pure center distance adaptation with an axial Feed of 0.4 mm per workpiece revolution. Figure 8 shows the workpiece flank topography simulation result over the 80% evaluation range. Due to the higher cross-axis angle and the resulting higher contact angles, considerable twist errors occur already with width crowning of 18 µm. Figure 9 shows the profile angle deviations resulting from the natural twist, the point-by-point numerically calculated kinematic adaptation required for the profile angle correction, and the approximated 4th-order trial function over the workpiece width.

The simulation of the workpiece flank topography for the process in Table 3 using the adaptive kinematics based on the approach functions from Fig. 9 is shown in Fig. 10. The maximum profile angle deviations are reduced from 8 to 1 µm and twist errors are thus quasi completely equalized. Furthermore, a simulative investigation of the cutting conditions with OpenSkiving was carried out at the uppermost and lowermost machining point. All local clearance angles are above 1°. At the lowest machining point, the meshing interference situation was checked and the absence of collisions was verified. Subsequently, the new kinematic adaptation was practically implemented with the boundary conditions from the testing of the process from Table 3. The tool was manufactured as all-tooth tool and has a level B quality according to DIN 1829. Figure 11 shows the tooth flank geometry evaluated on 14 flank lines. The maximum profile angle deviations produced in the practical trials are 2.5 µm. The remaining deviations do not show a twist, but are due to tool quality, machine control and operating misalignments and can be further reduced with improved tool quality. The simulative and practical equalization of the twist errors demonstrates the potential of the adaptive process control and can be applied in single-flank and two-flank gear skiving.

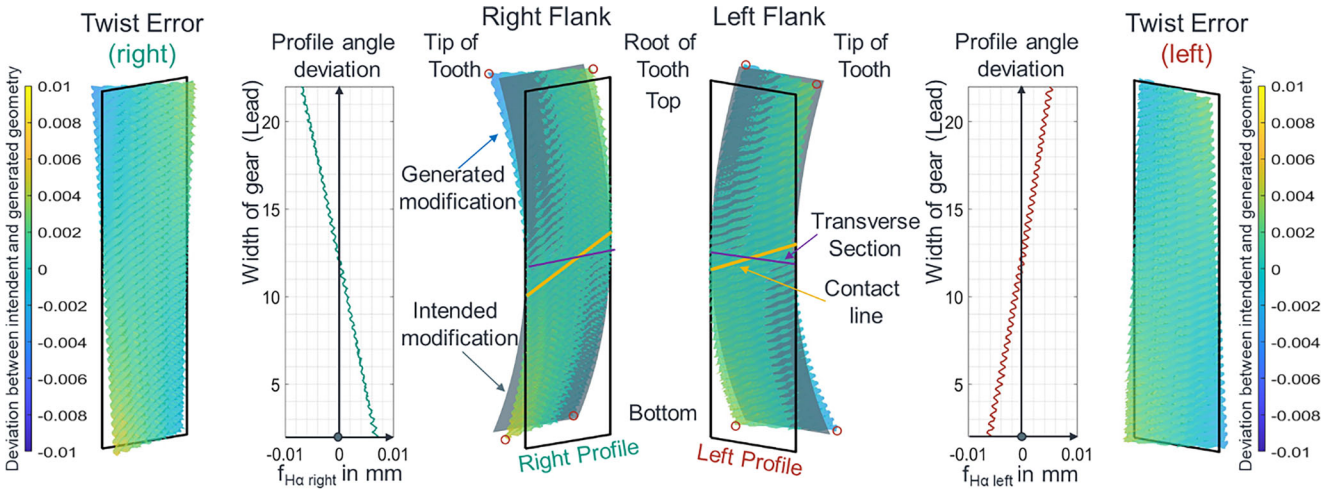

Fig. 8 Simulative natural twist analysis for process from Table 3

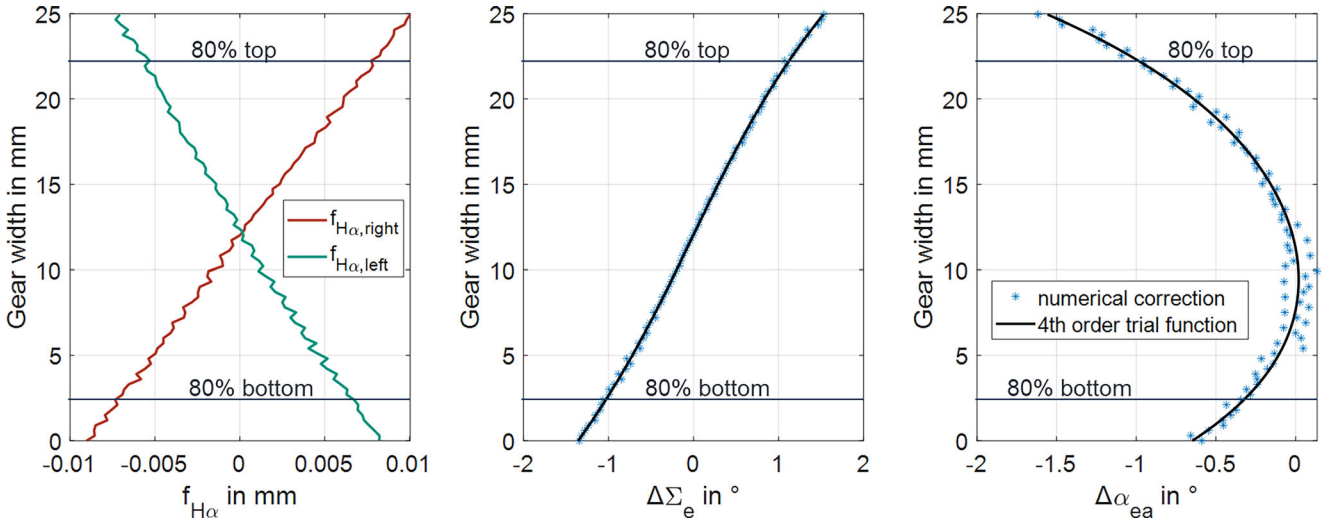

Fig. 9 Adaptive process kinematics for gear skiving based on the profile angle correction

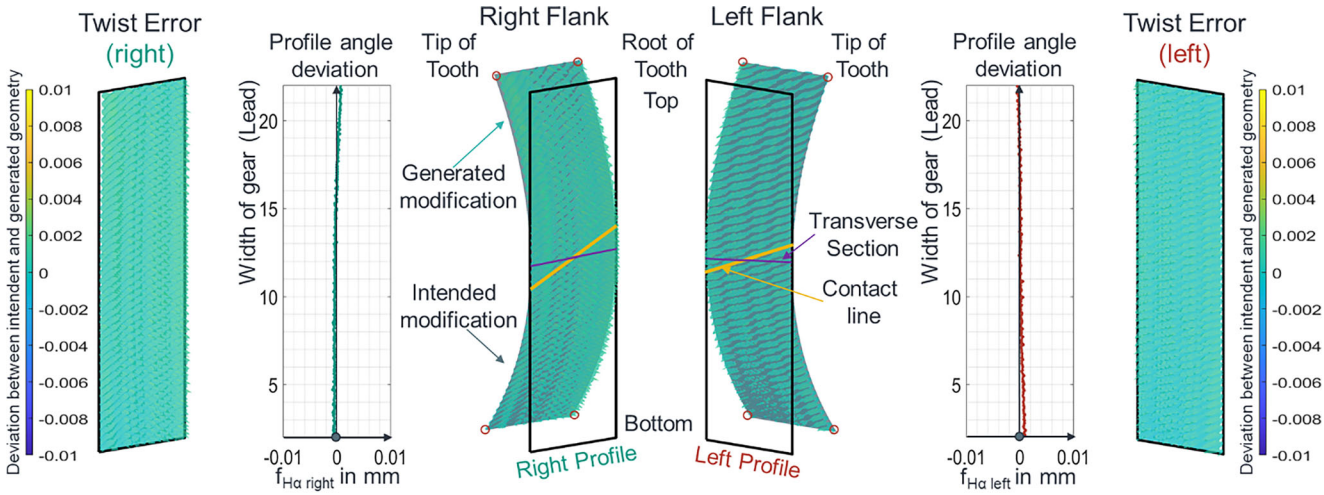

Fig. 10 Simulative twist analysis with adaptive process kinematics

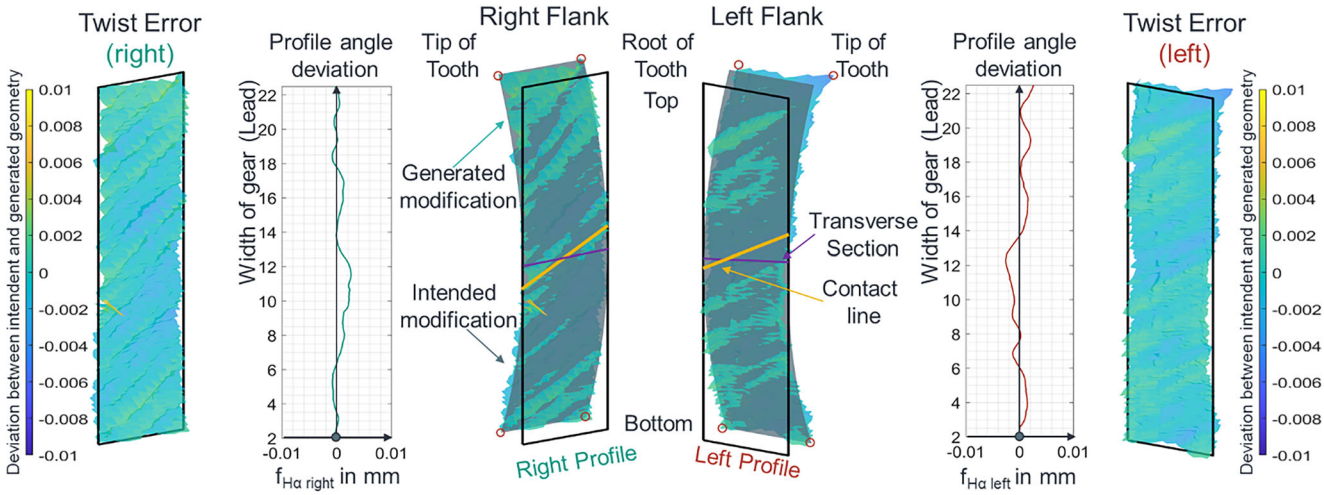

Fig. 11 Experimental twist analysis with adaptive process kinematics

11 Conclusion

Due to the continuous development of gear skiving, it is increasingly used for gear finishing, which raises the need for lead modifications without twist errors. In this work, a new tool design method based on the contact line between tool and workpiece was developed using the process characterization according to the conical helical generating gear. This method allows the design of tools with stair angle and constructive tip rake angle. For this purpose, a precise definition of the contact line through the inclination angle at the workpiece base cylinder was introduced as parameter for gear skiving. In the following, an investigation of the correlation between the contact line and design variables of the process and tool was done. By correlating the twist errors in gear skiving with the inclination of the contact lines, it is possible to specifically design processes for low-twist gear skiving. In addition to the reduction of the cross-axis angle, it is possible to minimize the twist, especially for a preferred flank, using the tools constructive tip rake angle as it was successfully validated in practical tests.

Finally, based on a new simulation method for predicting the manufactured gear flank topography, a new adaptive process kinematics over the workpiece width with 4th-order trial functions was developed, which enables low-twist gear skiving for any single- or two-flank processes with suitable tool design and thus fully qualifies gear skiving for modern gear fine machining. A simulation study with practical validation showed that with this method, twist errors can be quasi completely eliminated.

Funding Open Access funding enabled and organized by Projekt DEAL.

Conflict of interest A. Hilligardt and V. Schulze declare that they have no competing interests.

Open Access This article is licensed under a Creative Commons Attribution 4.0 International License, which permits use, sharing, adaptation, distribution and reproduction in any medium or format, as long as you give appropriate credit to the original author(s) and the source, provide a link to the Creative Commons licence, and indicate if changes were made. The images or other third party material in this article are included in the article's Creative Commons licence, unless indicated otherwise in a credit line to the material. If material is not included in the article's Creative Commons licence and your intended use is not permitted by statutory regulation or exceeds the permitted use, you will need to obtain permission directly from the copyright holder. To view a copy of this licence, visit http://creativecommons.org/licenses/by/4.0/.

References

1. Daniel B, Biermann T (2017) eAxle family in coaxial and offset arrangements. In: 16th CTI Symposium Automotive Transmissions, HEV and EV Drives, Berlin
2. Kleiber T (2019) DIN Q6 meets DIN Q10—Need for modern internal gear production. VDI-Berichte, vol 2355, pp 415–424
3. Weber G-T (2017) HARD SCUDDING – Trockene Hartfeinbearbeitung von Verzahnungen. In: Seminar Feinbearbeitung von Zahnrädern, WZL Aachen, 8.–9. November 2017
4. Li S, Kahraman A (2021) A scuffing model for spur gear contacts. Mech Mach Theory 156:104161
5. Lange J (2009) How are you dealing with the bias error in your helical gears. In: Proc. AGMA Fall Tech. Meeting, pp 47–54
6. Graf W (2017) Twist control grinding (TCG). Gear Technol 34(4):48–53
7. Winkel O (2010) New developments in gear hobbing. Gear Technol 27(2):45–52
8. Gravel G (2013) Simulation of deviations in hobbing and generation grinding. In: VDI International Conference on Gears, Munich
9. Hilligardt A, Schulze V (2022) A holistic approach for gear skiving design enabling tool load homogenization. CIRP Ann 71(1):85–88
10. Hilligardt A, Klose J, Gerstenmeyer M, Schulze V (2022) Modelling and prevention of meshing interference in gear skiving of internal gears. Forsch Ingenieurwes 86:673–681
11. Trübswetter M (2023) Geometrie des Wälzschälens (Dissertation)
12. Niemann G, Neumann B, Winter H (2011) Schraubrad-, Kegelrad-, Schnecken-, Ketten-, Riemen-, Reibradgetriebe, Kupplungen, Bremsen, Freiläufe vol 3. Springer, Berlin
13. Vargas B (2022) Wälzschälen mit kleinen Achskreuzwinkeln – Prozessgrenzen und Umsetzbarkeit (Dissertation)
14. KIT Campus Transfer (2023) OpenSkiving (1.77) [Software]. https://openskiving.kit-campus-transfer.de/. Accessed 20 July 2023
15. Bergmann B, Denkena B, Grove T, Picker T (2019) Chip formation of rounded cutting edges. Int J Precis Eng Manuf 20:37–44
16. Albert R (2019) Optimale Verzahnungsqualität durch prozesssicheres Spannen und Einstellen der Werkzeuge. In: 3. Fachseminar Wälzschälen. IWU Chemnitz